Proceedings of ASME GT2009
ASME Turbo Expo 2009: Power for Land, Sea, and Air
June 8-12, 2009, Orlando, Florida, USA

GT2009-59581

INFLUENCE OF INLET VELOCITY RATIO ON THE OUTLET FLOW UNIFORMITY OF A FAN-SHAPED FILM COOLING HOLE

James S. Porter*
School of Engineering
University of Tasmania
Hobart, Australia
jsporter@utas.edu.au

Alan D. Henderson
School of Engineering
University of Tasmania
Hobart, Australia
alan_dh@utas.edu.au

Gregory J. Walker
School of Engineering
University of Tasmania
Hobart, Australia
walkergj@utas.edu.au

ABSTRACT

Literature regarding the influence of inlet conditions on cooling hole flows is reviewed. A general failure to fully quantify inlet conditions and an inconsistent terminology for describing them is noted. This paper argues for use of an inlet velocity ratio (IVR) defined as the ratio of the coolant passage velocity to the jet velocity, together with additional parameters required to define the velocity distribution in the coolant supply passage.

Large scale experimental investigations of the internal flow field for a laterally expanded 50 times scale fan-shaped hole are presented, together with a computational investigation of the flow, for three inlet velocity ratios. Inlet lip separation causes a jetting effect that extends throughout the length of the cooling hole. A low velocity region of separated fluid exists on the downstream wall of the diffuser which deflects the jetting fluid towards the upstream side of the hole. This effect is most pronounced at low IVR values. The exit velocity profiles and turbulence distributions are highly dependent on the IVR.

NOMENCLATURE

L	Length of cooling hole
D	Diameter of cooling hole throat
M	Blowing ratio = $\rho_j U_j / \rho_\infty U_\infty$
Re	Reynolds number = $(\rho U D / \mu)$
Tu	Turbulence intensity
U	Time averaged velocity
IVR	Inlet Velocity Ratio = U_c / U_j
CVR	Cross-flow velocity ratio = $U_{c_{MEAN,90}} / U_{j_{MEAN}}$
P	Pressure
Cd	Discharge Coefficient = $\dot{m}_{ACTUAL} / \dot{m}_{IDEAL}$
$IFVR$	Inlet Friction Velocity Ratio = $u^* / U_{j_{MEAN}}$
u^*	Wall friction velocity = $\sqrt{\tau_0 / \rho}$
τ_0	Wall Shear Stress
ρ	Fluid density
μ	Dynamic viscosity
$\dot{m}$	Mass flow rate
U_c	Coolant passage velocity component in plane of cooling hole centerline
$U_{c,90}$	Coolant passage velocity component perpendicular to cooling hole centerline
U_j	Cooling hole throat mean velocity

SUBSCRIPTS

∞	mainstream
j	cooling hole jet
c	coolant supply passage
0	total
$MEAN$	area average

INTRODUCTION

The aim of film cooling is to create a uniform buffer film of cool air to protect turbine blade material from the very hot main gas flow. It is apparent from literature that optimum cooling per-

*Address all correspondence to this author.

formance can only be achieved through fine tuning of several flow parameters such as jet to mainstream mass flux (blowing) ratio, density ratio, mainstream and coolant Mach numbers, as well as geometric parameters such as hole shape, hole length, compound angle, and inclination angle. One important aspect of the cooling design that is critical to defining the internal cooling hole flow-field is that of the inlet conditions to the hole. It has been established by other workers that a plenum type inlet is not appropriate, in most cases, to model the true flow conditions in a typical turbine blade. Coolant supply passages within the blade are narrow: firstly for structural integrity, but also to promote increased passage velocities and thus higher heat transfer coefficients on the passage walls (Saumweber and Schulz [1]). In addition, the orientation of the supply passage flow relative to the cooling hole axis (or cross-flow angle) may vary, depending on the location within the blade, from 0 up to 180°. Over this range of inlet flow conditions there is a correspondingly large variation of the in-hole flow structure that cannot be overlooked as part of the overall film cooling design.

Studies from as early as 1969, such as those by Rohde et al. [2] and Hay et al. [3], have documented the effects of coolant passage cross-flow at the hole inlet on the discharge coefficient for cylindrical holes. Thole et al. [4], in their 1997 paper, were the first to present flow-field data for cylindrical holes using an experimental set-up that included a variable coolant cross-flow. Interest in the effects of internal coolant cross-flow has grown significantly in recent years and more studies have been published covering discharge coefficients, coolant flow-field, and cooling performance results for different inlet configurations.

In reviewing this literature, as detailed in the following section, it becomes apparent that there has been a distinct lack of consistency in terminology and specification of the coolant passage flow conditions. The majority of studies specify a coolant passage Mach number or Reynolds number, and a handful of studies provide a wall boundary layer thickness at a distance upstream of the hole inlet. However, none of these studies explicitly define the wall shear at the cooling hole entrance. In contrast, the flow conditions at hole exit have been well defined and specified in the majority of papers, with the commonly accepted blowing or mass flux ratio M being used in conjunction with exit cross-flow Mach number and boundary layer information. What is lacking for the coolant passage flow is information about the relationship between coolant and jet flows, and importantly, details on the velocity distribution on the inlet-side passage wall. The latter is critical to the development of the in-hole flow, as the size of the coolant passage boundary layer and wall velocity gradients will, within limits, determine the condition of the hole inlet flow.

One parameter which to this point has not been explicitly investigated for film cooling flows is that of the inlet velocity ratio (IVR), although the related inlet momentum ratio has sometimes been used, such as in Gritsch et al. [5]. The IVR will be defined here as the ratio of the coolant passage mean velocity component in the plane of the cooling hole centerline to the mean velocity in the cooling hole throat, $IVR = U_{c_{MEAN}}/U_{j_{MEAN}}$. There has been some confusion in terminology used by other workers when describing the coolant flow direction. It is more logical to define cross-flow as the velocity component normal to the cooling hole centerplane. To avoid confusion, this paper will use the term "cross-flow" in this sense. Pure cross-flow is then the case where the coolant passage orientation is perpendicular to the cooling hole centerline. The inlet flow situation may vary from co-flowing (0°cross-flow angle as in the present study), through pure cross-flow (90°), to counter-flow (180°).

The IVR alone is not enough to fully specify the approach flow conditions at inlet to the cooling hole. Accordingly, the wall friction velocity has been measured at 2 diameters upstream of the inlet to characterize the approaching coolant supply passage boundary layer. An inlet friction velocity ratio (IFVR) has also been defined as the ratio of wall friction velocity on the hole inlet wall to the mean velocity in the cooling hole throat $u^*/U_{j_{MEAN}}$. Of course, if the coolant supply passage flow were fully developed, the channel Reynolds number would suffice to determine the time-mean velocity distribution and wall shear of the approaching flow.

The cross-flow velocity ratio CVR, although not relevant for the present co-flowing inlet situation, can be defined as the ratio of the component of coolant passage mean velocity normal to the cooling hole center-plane to the cooling hole throat velocity, $CVR = U_{c_{MEAN,90}}/U_{j_{MEAN}}$. The coolant passage flow direction or cross-flow angle is therefore given by $\beta = \arctan(CVR/IVR)$.

The present study is believed to be the first to present detailed flow field measurements within a fan-shaped cooling hole. A large scale cooling hole model at 50 times scale permits this resolution. The combined experimental and numerical investigation is conducted for a co-flowing (0° cross-flow angle) coolant passage orientation. This situation is closely analogous to the hydrodynamic problem of flow in a flush-type inlet for a waterjet propulsor used on high speed ferry vessels, as reported by Brandner and Walker [6]. The results presented here provide a unique look at the in-hole flow-field, and reveal the effects of the inlet velocity ratio (IVR) on the in-hole flow development and thus the exit profile of the coolant. An associated computational fluid dynamics (CFD) investigation permits a greater understanding of the flow to be obtained.

LITERATURE REVIEW

A 1998 review by Hay and Lampard [7] examined published literature on discharge coefficients of film cooling holes and compiled an extensive list of investigations up to that time. The authors noted that the majority of work completed was experimental, with several including internal cross-flow effects, but little attention had been paid to shaped cooling holes. More

recently, Bunker [8] presented a comprehensive review of the state of film cooling research listing around 2700 related studies, mostly published since 1970. Bunker also observed that relatively little attention had been given to the effects of the internal coolant passage flow.

Previous studies of cooling hole inlet effects have employed parameters such as the coolant passage to jet "velocity head ratio" $(P_{0c}-P_j)/(P_{0c}-P_c)$ used to correlate discharge coefficient data by Rohde et al. [2], and the internal "jet-to-crossflow" momentum flux ratio $\rho_j U_j^2/\rho_c U_c^2$ used by Gritsch et al. [9]. For isothermal incompressible flows the latter reduces to the inverse square of the IVR used in the present investigation. Hay et al. [3] stated that the "velocity head ratio" was difficult to use with cross-flows on either side of the hole. Indeed, it seems the "standard" parameter for correlating discharge coefficient data among researchers is the pressure ratio P_{0c}/P_∞.

Hay et al. [3] published one of the first studies of the effects of cross-flows at inlet and exit of a cooling hole. They used a row of cylindrical holes ($L/D = 6, D = 10$ mm) supplied by a co-flow and a cross-flow coolant passage. The coolant passage Mach number was set and a general range of coolant Reynolds number provided. No coolant passage boundary layer information was included. Another paper by Hay and Lampard [10] examined discharge coefficients for fan shaped cooling holes with a co-flow coolant passage, but again specified only the coolant passage Mach number and pressure ratio across the hole.

A study by Thole et al. [4] was the first in open literature to look specifically at the effect of a co-flowing coolant passage on the exit flow field of a cylindrical cooling hole. The authors provided comprehensive details on the coolant passage flow, with Mach number, mean velocity, Reynolds number, and upstream boundary layer thickness being specified. Although not stated, the provided information enabled the tested IVRs to be calculated as 0, 1.2, and 2.0. The condition of the coolant passage boundary layer was not given, and the wall shear at the hole entry was not defined.

Kohli and Thole [11] performed a computational investigation for a forward-lateral shaped cooling hole with a plenum inlet, as well as coolant passage orientations of 0, 90 and 180° for a blowing ratio of $M = 1.0$. Although not stated explicitly, an IVR of 0.7 can be deduced for test cases where a coolant passage velocity existed at the hole inlet. Further work from Kohli and Thole [12] used CFD to investigate the effect of coolant passage Reynolds number and orientation for the same forward-lateral shaped hole geometry. The effect of coolant passage Reynolds number was investigated only for a 90° cross-flow and a blowing ratio of $M = 2$. Here again, the inlet velocity ratio was undefined and only the inlet wall boundary layer thickness was provided.

A series of papers by Gritsch et al. [5, 13, 14] examined discharge coefficients for both shaped and cylindrical cooling holes with a co- or cross-flowing coolant passage. The same test facility was used for these studies with parameters such as coolant passage Mach number, Reynolds number and turbulence intensity being specified. These studies make use of the internal momentum flux ratio, which is related to the IVR, giving a tested IVR range of $0-3$. A following paper from Gritsch et al. [15] looked at the effect of coolant passage Mach number on downstream cooling effectiveness, specifying the same parameters as in previous studies. In this case the internal momentum flux ratio was not used, so the range of tested IVRs cannot be determined. These studies give no information on the coolant passage boundary layer.

Adami et al. [16] presented a numerical study of the in-hole flow field for a cylindrical, fan-shaped, and laid-back hole with a 90° cross-flow at inlet. They examined the flow-field for one test configuration and specified only an external blowing ratio.

Kissel et al. [17] introduced ribs to a cross-flowing coolant passage and examined passage and main-flow Reynolds number effects on downstream surface cooling performance. The passage Reynolds number and hole pressure ratio were specified, but there were no details on the passage boundary layer (which would certainly have been influenced by the wall ribs) and insufficient data to determine the tested IVRs.

The most recent study that includes the effects of the coolant passage flow is that by Saumweber and Schulz [1]. This investigation looked at a cross-flowing coolant passage, and offered data for a range of coolant passage Mach numbers and blowing ratios for a fixed exit cross-flow Mach number. Again, the IVR was not quantified, but could be calculated from data provided. Tests covered a range from $0-3.5$ at the highest coolant passage Mach number of 0.59 for a blowing ratio of 1.0.

General findings from previous research

Despite an obvious increased interest in the effects of coolant passage flow on film cooling in the past decade, it is evident that the works published to date have in the majority of cases failed to provide details on the IVR and the incoming boundary layer condition in the coolant passage. Although this complicates the direct comparison of results from different researchers, several common key points regarding the inlet flow have been identified.

The most prominent inlet flow phenomenon is that of separation from the inlet edge of the cooling hole. The typical 30° inclination angle of cooling holes changes the inlet flow considerably from that of a sudden contraction or orifice type flow, as discussed by Hay et al. [3]. Work by Pietrzyk et al. [18] presented exit velocity and turbulence information for an inclined cylindrical hole fed by a plenum inlet. The skewed exit profile of the jet led to the conclusion that a separation region must exist on the downstream side of the cooling tube as a result of the large turning angle. A numerical study by Leylek and Zerkle [19], replicating the work of Pietrzyk et al., predicted the existence of this separated region and associated jetting of fluid towards the

upstream side of the exit. Further works of Thole et al. [4], Kohli and Thole [11], Kohli and Thole [12], Gritsch et al. [13], Kissel et al. [17], and Saumweber and Schulz [1], have discussed this inlet separation and implied from exit data or numerical predictions that such a separation exists. There has been no full field experimental data presented from within the hole to confirm this so far.

Stagnation Point The location of the stagnation point at the hole entrance is critical in defining the location and extent of the separated region. Hay et al. [7] noted this in relation to understanding the variation of discharge coefficients, stating that as the coolant passage mean velocity (in the present terminology) increases, the stagnation point moves upwind to the downstream inlet edge, and then into the hole at still higher cross-flow velocities. This is in line with a study by Brandner and Walker [6] who experimentally investigated a flush mounted water jet propulsor inlet, commonly used in high speed ferries. Brandner and Walker found that incidence angle on the inlet lip has significant effect on non-uniformity at the duct exit, with large velocity gradients for low and high IVRs. As IVR was increased from 0 to 3, the stagnation point, measured by lip static tappings, progressed from outside to inside the duct. In addition, the DC60 parameter, used to quantify distortion at the duct outlet, showed an almost linear variation with IVR over the range from $1-2$, with minimum distortion at an IVR of 1. Indeed, all studies incorporating coolant passage cross-flow have noted a significant alteration of exit flow-field, cooling performance, or discharge coefficients with varying coolant passage Mach number or Reynolds number.

The literature review presented here effectively covers the current offerings of experimental and computational investigations into the effects of flow at the cooling hole inlet. It can be seen that the inlet velocity ratio has not been previously defined for film cooling flows, despite its importance in defining the in-hole flow. Several studies, such as Saumweber and Schulz [1], Thole et al. [4] and Gritsch et al. [14] have hinted at the implications of such a ratio, but have not characterized the flow in terms of IVR. An important point to note is that experiments conducted by increasing the blowing ratio for a fixed exit flow and fluid density must produce associated changes in the IVR: thus the results obtained must depend on the combined effects of blowing ratio and IVR, and it is therefore incorrect to attribute the observed changes to the influence of blowing ratio alone.

EXPERIMENTAL FACILITY AND INSTRUMENTATION

The low speed wind tunnel at the University of Tasmania that was used for this research is shown schematically in Fig. 1. This facility achieves similarity with aeroengine turbine blade values for numerous flow parameters, including mainstream and coolant passage Reynolds numbers, jet to mainstream mass flux

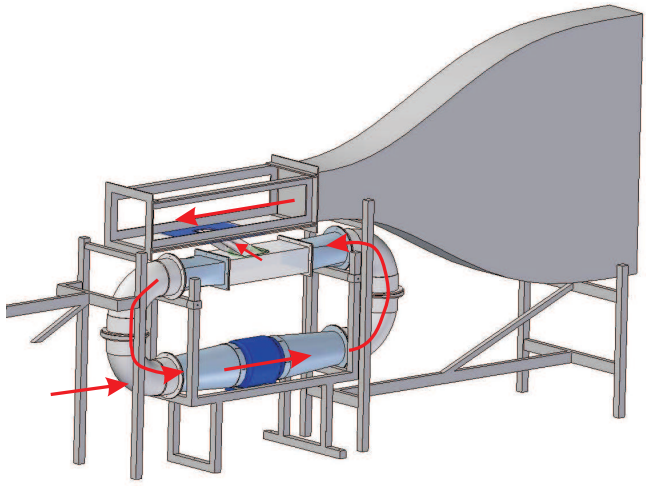

Figure 1. WORKING SECTIONS OF TEST FACILITY. ARROWS INDICATE FLOW DIRECTION

(blowing) ratio M, and geometric parameters as shown in Table 1. The wind tunnel is an open circuit design using an axial flow fan to draw air through the main working section. As shown in Fig. 1, there are two working sections connected by the film cooling hole model, each drawing air from atmosphere. Both of these can be traversed by probes to take measurements of the flow, and are constructed from clear acrylic. The main section, representing the hot gas path over the surface of a turbine blade, is 1000 mm long and 225×225 mm in cross-section, and is preceded by a smooth two-dimensional contraction. The boundary layer is tripped 200 mm upstream of the working section inlet to ensure a fully developed turbulent boundary layer through the working section. Mainstream turbulence intensity of 0.6%, a maximum mainstream velocity of 20 ms^{-1}, flow direction uniform to within $\pm 0.5^\circ$, and velocity uniform to within $\pm 0.5\%$ is achievable.

The design of the facility, as detailed in Porter et al. [20], en-

Parameter	Engine value	Test value
D (hole diameter)	$0.7-1.2$ mm	50 mm
α (inclination angle)	$20-60^\circ$	30°
L/D	$3-6$	5
Fan expansion angle	$14-32^\circ$	30°
DR (density ratio)	$1.5-2$	1
VR (ext velocity ratio)	$0.5-2$	$0.5-1.9$
M	$0.8-4$	$0.5-1.9$
I	$0.9-2$	$0.25-2.25$
Re_{D_j}	$1-3\times10^4$	3×10^4

Table 1. COMPARISON OF ENGINE AND EXPERIMENTAL PARAMETERS FOR CURRENT STUDY

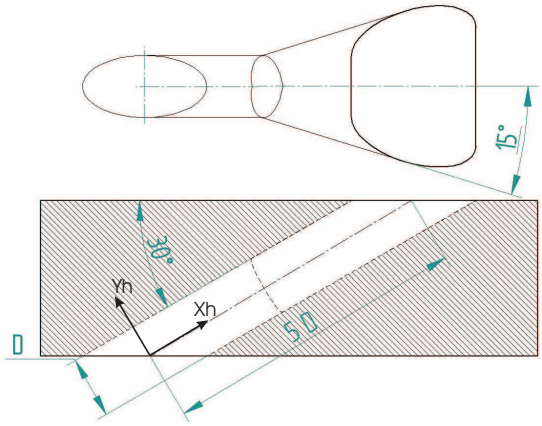

Figure 2. FAN-SHAPED COOLING HOLE GEOMETRY

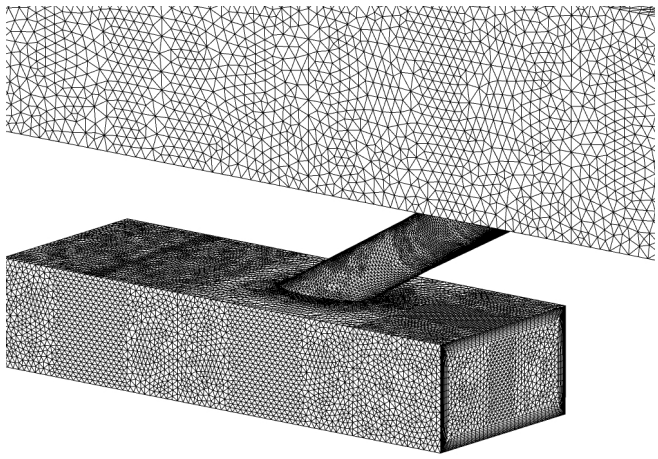

Figure 3. COMPUTATIONAL MESH

ables independent control of flow conditions in the coolant passage, cooling hole, and mainstream, in a similar fashion to the facility described by Wittig et al. [21]. This is achieved through a re-circulating coolant loop driven by an axial fan, and a secondary radial flow fan (not shown) to supply and control make-up air that exits through the cooling hole. The mass flow rate of this additional jet fluid is measured by a calibrated nozzle with an uncertainty of less than 2%. Figure 2 shows the cooling hole geometry tested in the present study. It is a typical laterally expanded fan-shaped cooling hole, with $L/D = 5$, and a metering (throat) length of $L/3$. The included angle of the diffuser section is 30°. A novel aspect of this work is the 50 times scale cooling hole geometry which allows aerodynamic probes access for detailed measurements. The metering section diameter (D) of the cooling hole model is 50 mm. Blowing ratios of 0.5 and 1.0 are tested in this study, together with inlet velocity ratios of 0.3, 0.6, and 0.9 for a co-flowing (0°) coolant passage orientation.

Velocity and turbulence intensity measurements were made using a single sensor Dantec type 55P11 miniature hot wire probe with wire axis normal to the average mainstream flow direction. The probe was operated by a TSI IFA100 constant temperature anemometer with standard bridge, and calibrated in situ against a Pitot-static tube in the plane of the sensor tip. Turbulence intensity values were calculated from the measured root-mean-square (rms) velocity fluctuations scaled by the mean velocity value at the measurement location. Measurements were corrected for electrical noise in the anemometer.

COMPUTATIONAL MODEL

The computational domain was divided into 7 regions to allow independent mesh controls to be applied to each. All regions were meshed using a hybrid method consisting of tetrahedral elements in the far wall flow and inflated prismatic elements in the near wall flow to improve boundary layer modeling. The total number of elements was approximately 1.8×10^6. The mesh can be seen in Fig. 3.

The near wall flow was modeled using "automatic" wall functions, which automatically switches between a low Reynolds number approach to scalable wall functions depending on local conditions and the wall normal element spacing [22]. The y+ value of the mesh element adjacent to the wall varied between 10 - 50 in all cases. Post processing showed that the boundary layer was resolved by around 10 elements, as recommended in the software documentation for the code used, which was CFX 11.0 [22].

The Shear Stress Transport (SST) turbulence model was used for turbulent closure as it is regarded as one of the better two-equation turbulence models at predicting separation in an adverse pressure gradient [22]. A second order accurate advection scheme was used. The six equations solved were u, v and w-momentum equations, and conservation of mass, turbulent kinetic energy (k) and turbulent frequency (ω). A convergence criterion for maximum RMS residual of 10^{-6} was set, which is two orders of magnitude below the default level used by the solver [22]. The solution times were generally around 3 hours using 10 processors of a SGI ALTIX 4700 system (64-bit Itanium 2, 1.6 GHz).

EXPERIMENTAL RESULTS

Contour plots of normalized velocity $U/U_{j_{MEAN}}$ and turbulence intensity U_{RMS}/U for IVR values of 0.3, 0.6 and 0.9 are presented in Fig. 4. $U_{j_{MEAN}}$ is defined as the mean velocity through the throat of the hole. This quantity was held constant at 9 ms^{-1} for all tests, and the corresponding Reynolds number at standard conditions was 3×10^4. The mainstream velocity, U_∞, was held constant at 18 ms^{-1} with $M = 0.5$; for $M = 1.0$ the

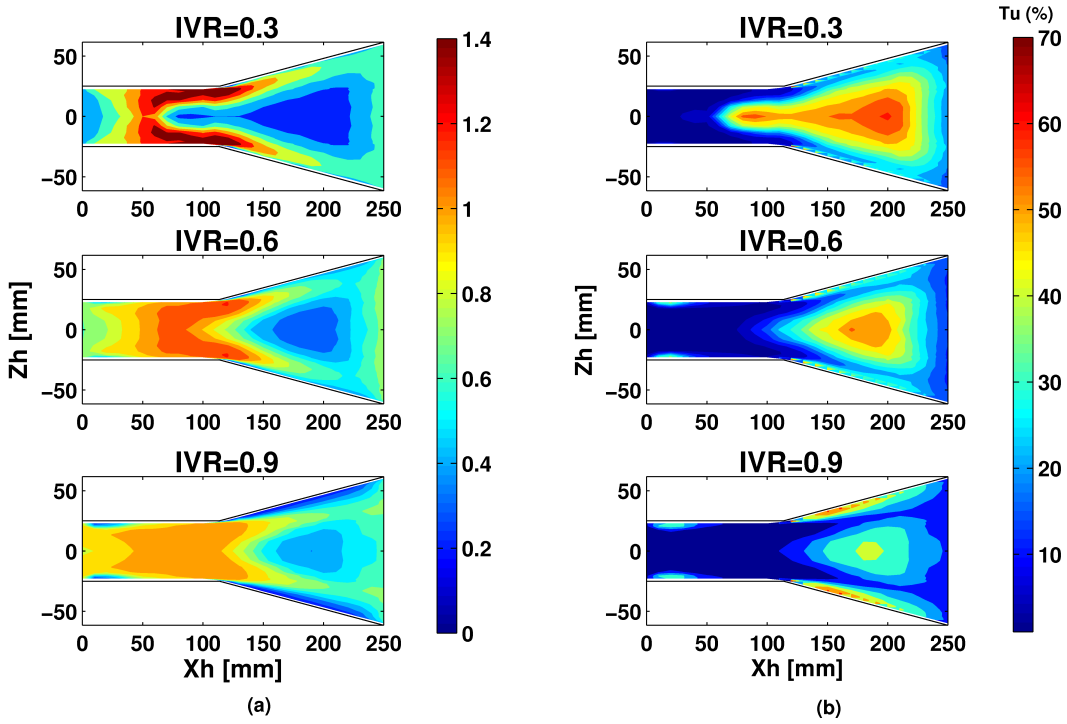

Figure 4. CONTOURS OF (a) NORMALISED MEAN VELOCITY AND (b) TURBULENCE INTENSITY ON PLANE Yh=0, FOR BLOWING RATIO M=0.5

value of U_∞ was 9 ms^{-1}. The measurement plane is located along the hole centerline and oriented in a lateral direction. Figure 2 shows the hole coordinate system, subscripted h, with origin at the center of the hole inlet plane, and X_h axis aligned with the hole centerline. The measurement plane is thus in the $X_h - Z_h$ plane at $Y_h = 0$. Results presented here are for one half of the hole with the data mirrored to provide better visualization of the flow pattern. It should be noted that the single axis hot-wire sensor detects an effective velocity which represents a vector sum of individual velocity components normal to the sensor. For measurements here, the sensor was aligned in the mid-plane normal to the hole axis, and parallel to the side wall. There is an associated uncertainty in the experimental turbulence values, which essentially indicate the velocity fluctuation component perpendicular to the hot-wire sensor.

The normalized velocity contours reveal a distinct change in flow pattern within the hole as the IVR is increased from 0.3 to 0.9. At an IVR of 0.3 there is a marked inlet lip separation that produces a region of high velocity fluid starting midway along the throat and splitting either side of a central low velocity region at the throat outlet. The maximum throat velocity in the inlet has a normalized value of more than one, demonstrating that considerable acceleration of the flow has occurred due to the blocking effect of the inlet separation. As the flow reaches the diffuser section, the flow decelerates; but the higher velocity region continues to hug the lateral walls of the hole as the low velocity region dramatically increases to fill the majority of the diffuser. Velocities in this region are approaching zero, indicating that there is incipient re-circulation of fluid in this region.

As the IVR is increased to 0.6 there is a reduction in peak fluid velocity, but still a similar pattern with higher velocity fluid deflected to the sides of the diffuser around a central low velocity blockage. At IVR=0.9 the effect is reduced further, to the extent that the higher velocity fluid does not follow the diffuser walls as closely and low velocity fluid occupies the near wall region. The associated turbulence intensity contours reveal that the low velocity region produced by the cooling hole inlet separation is highly turbulent and occupies a large percentage of the diffuser space in the measurement plane, particularly for the low IVR case. As with the velocity contours, the turbulence intensity contours show a progressive variation as IVR is increased. The highly turbulent region in the diffuser becomes smaller and less intense at higher IVR, and the flow near the walls of the diffuser starts to show high turbulence, indicating some separation from the start of the diffuser section.

COMPUTATIONAL RESULTS

Further insight into the flow structure can be gained from examination of the results from the computational simulation.

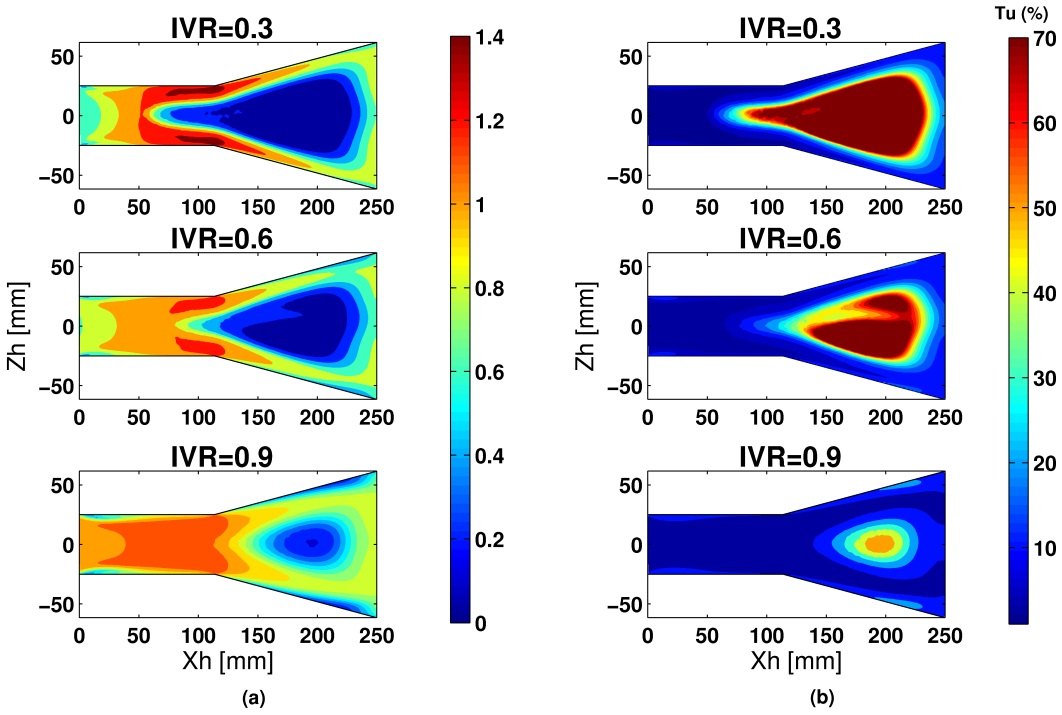

Figure 5. COMPUTED CONTOURS OF (a) NORMALISED VELOCITY AND (b) TURBULENCE INTENSITY ON PLANE Yh=0, FOR BLOWING RATIO M=0.5

Firstly, a comparison of velocity contours in Figs 4 and 5 shows good qualitative agreement with the experimental measurements, with the same high velocity region splitting at the start of the diffuser around a large region of low velocity fluid. A brief investigation of variations in the height of the Y_h plane cut demonstrated quite high sensitivity of the velocity distribution, which is a possible source of slight differences in the plots. The progression of flow patterns is also strikingly similar to experiment, with the simulation showing the same region of low velocity fluid near the diffuser walls at $IVR = 0.9$.

The computed turbulence intensity values were derived from the turbulent kinetic energy by making the assumption of isotropic turbulence. Although the turbulence will exhibit some anisotropy, the resulting computed distribution still gives a useful indication of the streamwise turbulence intensity measured by the hot wire sensor. The similarity to the experimental data is good, though there is perhaps a slight over-prediction of the turbulence intensity in the central diffuser region. This could be due to the very low velocities in the diffuser in the computed solution. The patches of high turbulence in the near wall region at the start of the diffuser, present in the experimental results, are not evident here.

Further validation of the numerical results can be obtained by comparing normalized velocity profiles along the cooling hole centerline. Figure 7 presents the measured and computed velocity profiles at $Xh/D = 2.2$ and 3.8 for $IVR = 0.9$ and $M = 0.5$. The similarity of the profiles at $Xh/D = 2.2$ is good; at $Xh/D = 3.8$ there is still good agreement. The inability of the turbulence model to fully capture the effects of the adverse pressure gradient and increased turbulence level in the diffuser may be cause for the discrepancies. The good agreement of the computational results with experiment provides confidence in the solution for the entire flow field, which will be examined in the following discussion.

ANALYSIS OF FLOW DYNAMICS

In-Hole Flow Field

Figure 6 shows velocity magnitude vectors in the $Z = 0$ plane through the hole for the IVRs tested. These images indicate a prominent jetting of the coolant fluid originating from the downstream lip of the hole inlet. This jetting effect has been shown by previous numerical simulations such as those of Kohli and Thole [11] and Leedom and Acharya [23]. These workers found the effect to be most prominent for plenum inlet or low coolant passage velocity cases, which correspond to low IVR values. Figure 6 demonstrates that the strength of the jetting region decreases with increasing IVR. Streamlines from the computed results show a roll-up of fluid from the sides of the hole inlet into a pair of counter rotating vortices in the throat section. The

height of these vortices directly affects the strength of the jetting region: at low IVR, the vortices occupy over half the tube height at the start of the diffuser, pushing the jetting fluid to the upstream wall and causing increased local velocities.

The adverse pressure gradient imposed by the diffuser creates a tendency for the flow to separate. In the current case, however, the flow is already split due to separation at the inlet. The adverse pressure gradient acts to disperse the vortices, creating a separation bubble on the center of the downstream diffuser wall. This forces the jetting fluid to remain near the upstream side of the hole, but also to deflect laterally around the separated fluid and remain attached to the diffuser side walls. This behavior contrasts with the typical wall separation observed at the entrance of a two-dimensional diffuser with a large area ratio; it is a combined result of the jetting effect produced by the inlet lip separation and the associated separation on the downstream wall of the diffuser entrance. Saumweber and Schulz [24] and Adami et al. [16] also identified the downstream wall separation bubble in their numerical results. Saumweber and Schulz used this flow feature to explain the typical bi-modal pattern of cooling effectiveness surface distributions downstream of the fan-shaped hole exit. Peak effectiveness values at the lateral sides of the surface distribution agree with the deflection of the in-hole flow around the separation bubble. Saumweber and Schulz proposed that such a separation is beneficial to cooling performance as it promotes lateral spreading of the coolant.

Centerline Velocity Profile Comparisons

Velocity profiles at $Z = 0$ for each of the three IVRs tested are presented in Figure 7. The decrease in height of the separated region on the downstream wall of the throat as IVR is increased can be clearly seen from these plots. The jetting region of high velocity fluid is prominent in the upstream portion of the hole, with the maximum peak velocity occurring for the lowest IVR case. Turbulence intensity plots not presented here show that the peak turbulence occurs in the region of highest velocity gradient dU/dy, consistent with findings of Andreopoulos and Rodi [25] and Pietrzyk et al. [18] at the exit plane for a normal round jet.

Contours of velocity at the same Xh/D locations, presented in Fig. 8 reveal further information about the nature of the cooling hole flow. In the throat ($Xh/D = 2.2$), the contours clearly show the vortex pair discussed above; these closely resemble the kidney-shaped vortex seen downstream of a cylindrical jet in cross-flow. These vortices persist into the diffuser, where they spread and reduce in intensity. Vector plots indicate some very low velocity fluid in this region suggestive of incipient flow recirculation. The reduction in height and size of the vortex pair structure with increasing IVR is evident from these images.

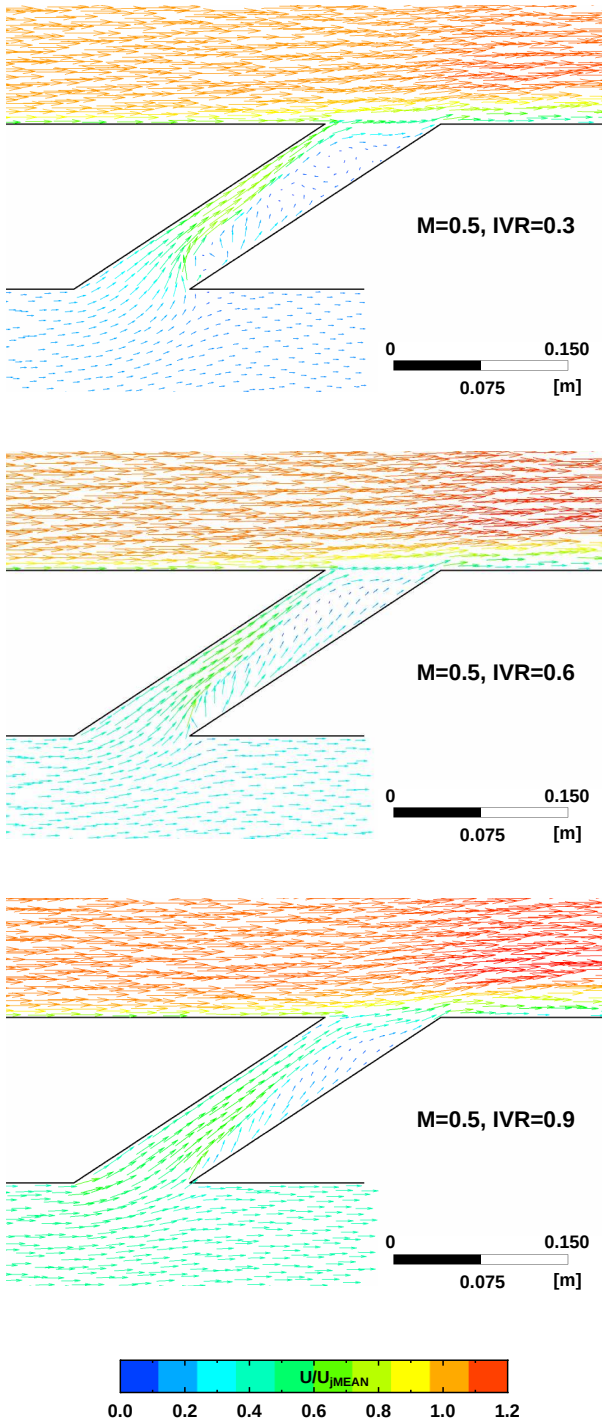

Figure 6. VELOCITY VECTORS IN THE CENTERLINE (Z=0) PLANE FOR DIFFERENT IVR

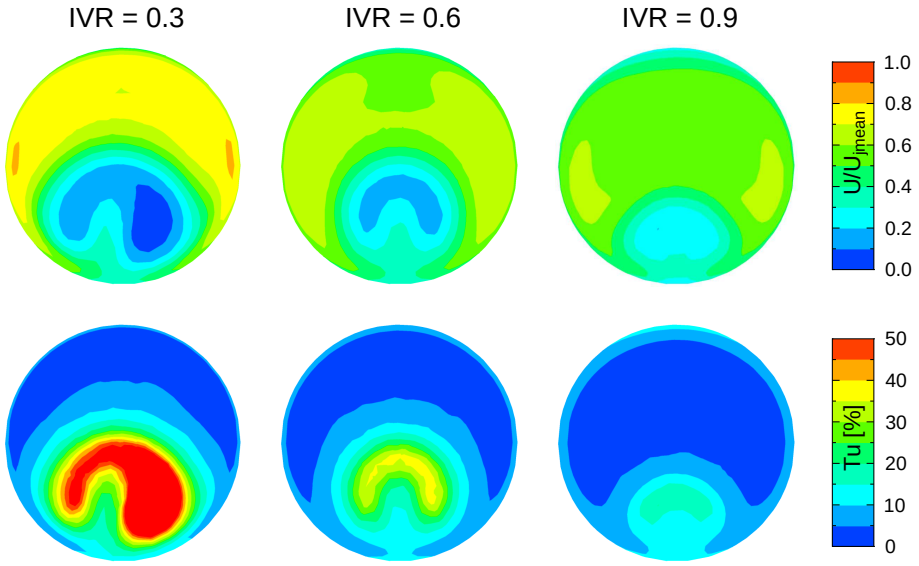

Figure 8. CONTOURS OF NORMALIZED VELOCITY AND TURBULENCE INTENSITY IN HOLE THROAT LATERAL PLANE. Xh/D=2.2 M=0.5

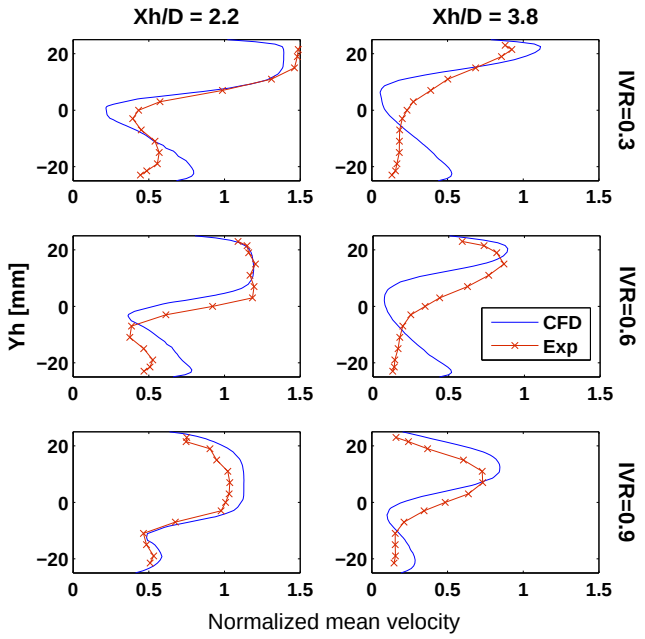

Figure 7. COMPARISON OF NORMALIZED VELOCITY PROFILES IN HOLE CENTERPLANE. Zh=0, M=0.5

Effect of Blowing Ratio

To examine the effect of blowing ratio on the cooling hole flow, tests were done at a blowing ratio of $M = 1.0$ by adjusting the mainstream velocity alone. Figure 9 shows contour plots for an IVR of 0.6 at blowing ratios of 0.5 and 1.0 from measurement and computation. The flow fields for these two blowing ratios are essentially similar, demonstrating that blowing ratio alone has little influence on the in-hole flow. Changes in flow structure with blowing ratio generally result from a change in cooling hole Reynolds number as the pressure ratio is adjusted to achieve the desired blowing ratio.

DISCHARGE COEFFICIENTS

Values of discharge coefficients Cd (defined as the ratio of actual to ideal cooling hole mass flow) were derived from the measured data for IVR cases of 0.3, 0.6, and 0.9 and plotted in Fig. 10. The trend of increasing Cd with IVR is immediately obvious. A similar trend was found by Gritsch et al. [5] with varying coolant passage Mach number for an external flow Mach number of 0. Their results showed a peak in discharge coefficients for a particular coolant passage Mach number. Gritsch et al. [14] presented normalized discharge coefficient data for cylindrical holes in terms of the internal momentum flux ratio, and for a co-flowing coolant passage showed a peak Cd at a momentum flux ratio of about 1. This result can be explained through the increasing contribution of the coolant passage flow dynamic pressure, and a reduction in the extent of the separated region as the stagnation point moves upstream to the hole inlet lip. Thole et al. [4] and Gritsch et al. [13] made similar deductions on the basis of their experimental observations. It is expected that extension of the present measurement range of IVRs would also reveal a "peak" IVR for which the discharge coefficient reaches a maximum. The maximum practical value of IVR will be determined by the limit at which blow-off of the emerging coolant jet occurs; depending on the cooling hole geometry, this limit may

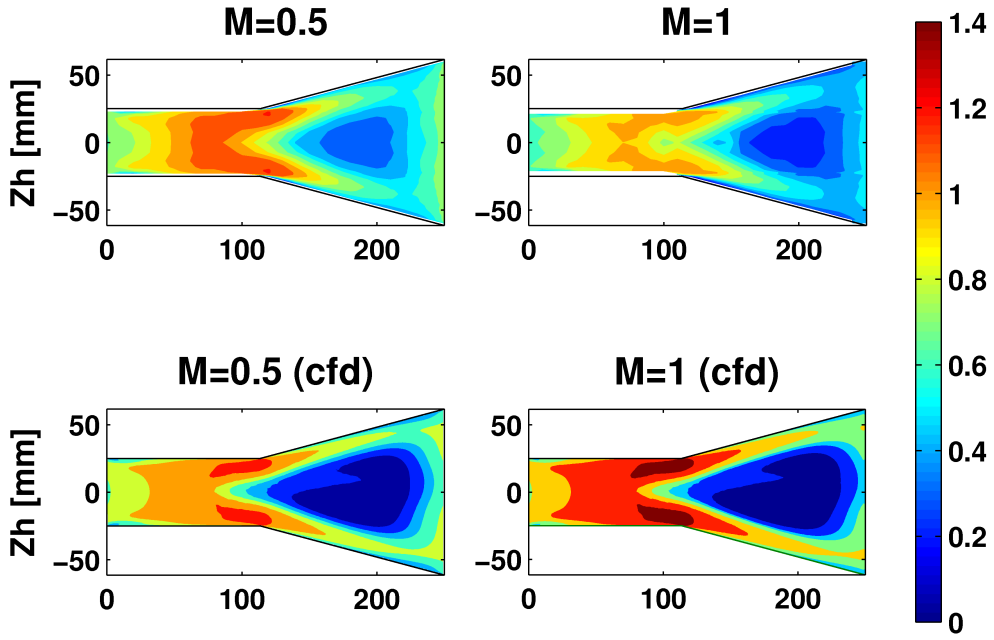

Figure 9. COMPARISON OF VELOCITY CONTOURS FOR A BLOWING RATIO OF M=0.5 (left) AND 1.0 (right). IVR=0.6.

be reached before the Cd value attains a maximum.

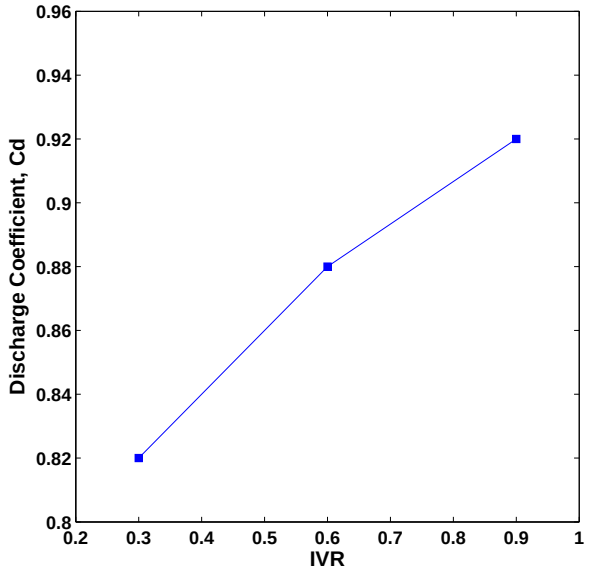

Figure 10. VARIATION OF DISCHARGE COEFFICIENT WITH INLET VELOCITY RATIO

DISCUSSION

The present results clearly demonstrate the influence of IVR on the in-hole flow field and discharge coefficients for a fan-shaped cooling hole with co-flowing coolant passage at inlet. As the mainstream and cooling hole flows were held constant for all tests, the observed behavior must be primarily attributed to changes in the IVR. It seems, from the few studies for which an IVR can be determined from the published data, that maxima of discharge coefficient values and exit velocity uniformity, and minimum exit turbulence levels can be expected at an IVR close to 1. This value of IVR positions the stagnation point close to the center of the inlet lip and minimizes separation at the cooling hole entry. The present results of in-hole velocity contours and profiles demonstrate the development of a more uniform in-hole flow as the IVR increases. Waterjet propulsor inlet measurements by Brandner and Walker [6] further support this con-

	$\delta/\mathbf{D}$	**IFVR**	$\mathbf{Re_{D_c}}(\times\mathbf{10^{-4}})$
$IVR = 0.3$	0.143	0.026	0.9
$IVR = 0.6$	0.157	0.103	1.8
$IVR = 0.9$	0.161	0.178	2.5

Table 2. COOLANT PASSAGE BOUNDARY LAYER CONDITION AT INLET

clusion, reporting the lowest flow distortion at the duct exit for an IVR of 1. Brandner and Walker also examined the effect of approach flow boundary layer thickness with tests for total thicknesses of 13.3% and 30% of the inlet duct diameter. The thicker boundary layer reduced both the strength of secondary flow in the duct and the distortion of velocity distributions at the duct exit.

These results emphasize the need for a full specification of the approaching coolant passage flow. Coolant passage boundary layer data for the present tests are presented in Table 2. The boundary layer thickness in the present study varies only slightly across the three test cases, between 14% and 16% of the inlet diameter. The wall friction velocity upstream of the hole inlet shows a much greater variation with the IVR.

The limiting cases for condition of the coolant passage flow are inviscid flow, and fully developed passage flow. For the former case the passage flow can be fully defined by the IVR for incompressible flow, or a momentum ratio for compressible flow. For the latter case the velocity distribution near the wall can be solely determined from knowledge of the passage Reynolds number or wall friction velocity ratio. In the general case, the coolant passage flow will not be fully developed and a boundary layer will be present on the passage wall preceding the hole inlet. Full specification of the flow condition approaching the inlet will then require knowledge of both the boundary layer thickness and boundary layer Reynolds number.

If the hole inlet diameter is sufficiently small for the inlet flow to be totally drawn from the wall similarity region of the boundary layer, specification of the wall friction velocity of the approaching flow should be sufficient to determine the inlet flow behavior. Where the boundary layer thickness is comparable with the hole diameter, the ratio of these two lengths also becomes relevant, and the velocity distribution of the whole boundary layer region needs to be defined.

In summary, a comprehensive description for all possible flow regimes requires in general, the wall friction velocity ratio (IFVR), the passage Reynolds number or boundary layer Reynolds number of the approach flow, and ratio of boundary layer thickness or passage half width to the cooling hole inlet diameter. The combination actually required will depend on the specific geometry and operating conditions.

CONCLUSIONS

The turbine blade cooling problem is principally concerned with the flow distribution at exit from the cooling hole, and the manner in which this influences the heat transfer on the surrounding blade surface. It has become increasingly apparent that the cooling hole exit flow is strongly dependent on conditions at the hole entrance, which are in turn dependent on the flow distribution in the coolant supply passage. For a co-flowing supply passage and cooling hole configuration, as studied in the present investigation, the degree of flow separation at the cooling hole inlet is strongly influenced by the ratio of the coolant supply passage velocity to the cooling hole jet velocity (or inlet velocity ratio IVR).

The IVR therefore becomes an important parameter for cooling system design. Previous studies, together with the present investigation, indicate that the degree of flow separation from the cooling hole inlet lip, and therefore the associated flow distortion at the cooling hole exit, are both minimized at IVR values of around unity.

Specification of the approaching flow distribution in the coolant supply passage will require additional parameters such as the passage Reynolds number, if the flow is fully developed, or inlet wall boundary layer thickness and Reynolds number where the supply passage has a uniform core flow. An extensive literature review has indicated that this data is lacking in previous publications on this subject; the data is either incomplete or not explicitly specified.

The present detailed study of in-hole flow behavior for a typical fan-shaped cooling hole geometry has shown that computational predictions replicating measured coolant supply passage inlet conditions gave useful descriptions of the in-hole flow behavior. The extent of lip separation and associated jetting at the hole entrance was found to be strongly influenced by the IVR value. The associated low velocity region at the center of the diffuser entrance caused the flow to remain attached to the side walls of the exit fan.

The situation will be more complex for a cross-flow situation where there is a component of the coolant supply passage velocity normal to the cooling hole center plane. An additional inlet velocity ratio based on the cross-flow velocity component will be required in this situation. A variety of terminology has been used in previous publications to describe internal cross-flow effects, and a more consistent approach would be desirable to reduce the potential for confusion and facilitate comparison between different studies. The present publication has made some suggestions in this regard.

ACKNOWLEDGEMENTS

The authors gratefully acknowledge support from Rolls-Royce plc UK for financial assistance. ANSYS is thanked for the provision of an academic license for the CFX 11.0 suite. The authors appreciate helpful comments by reviewers of the draft paper.

REFERENCES

[1] Saumweber, C., and Schulz, A., 2008. “Comparison of the cooling performance of cylindrical and fan-shaped cooling holes with special emphasis on the effect of internal coolant

cross-flow". In Proc. ASME Turbo Expo 2008, GT2008-51036, June, Berlin, Germany.
[2] Rohde, J., Richard, R., and Metger, G., 1969. "Discharge coefficients for thick plate orifices with approach flow perpendicular and inclined to orifice axis". *NASA TN D-5467*.
[3] Hay, N., Lampard, D., and Benmansour, S., 1983. "Effect of crossflows on the discharge coefficient of film cooling holes". *Journal of Engineering for Power,* **105**(2), pp. 243–248.
[4] Thole, K., Gritsch, M., Schulz, A., and Wittig, S., 1997. "Effect of a crossflow at the entrance to a film-cooling hole". *ASME Journal of Fluids Engineering,* **119**(3), pp. 533–540.
[5] Gritsch, M., Schulz, A., and Wittig, S., 1998. "Discharge coefficient measurements of film-cooling holes with expanded exits". *ASME Journal of Turbomachinery,* **120**(3), pp. 557–563.
[6] Brandner, P., and Walker, G., 2007. "An experimental investigation into the performance of a flush water-jet inlet". *Journal of Ship Research,* **51**(1), pp. 1–21.
[7] Hay, N., and Lampard, D., 1998. "Discharge coefficient of turbine cooling holes: A review". *ASME Journal of Turbomachinery,* **120**(2), pp. 314–319.
[8] Bunker, R. S., 2005. "A review of shaped hole turbine film-cooling technology". *ASME Journal of Heat Transfer,* **127**(4), pp. 441–453.
[9] Gritsch, M., Schulz, A., and Wittig, S., 1998. "Method for correlating discharge coefficients of film-cooling holes". *AIAA Journal,* **36**(6).
[10] Hay, N., and Lampard, D., 1995. "The discharge coefficient of flared film cooling holes". In Proc. International Gas Turbine & Aeroengine Congress & Exposition, June 5-8, 1995. 95-GT-15.
[11] Kohli, A., and Thole, K., 1997. "A CFD investigation on the effects of entrance crossflow directions to film-cooling holes". In ASME Heat Transfer Division, (Publication) HTD, Vol. 350, pp. 223–232.
[12] Kohli, A., and Thole, K., 1998. "Entrance effects on diffused film-cooling holes". In ASME International Gas Turbine & Aeroengine Congress & Exhibition, Jun 2-5 1998. Paper 98-GT-402,, American Society of Mechanical Engineers (Paper), p. 8.
[13] Gritsch, M., Saumweber, C., Schulz, A., Wittig, S., and Sharp, E., 2000. "Effect of internal coolant crossflow orientation on the discharge coefficient of shaped film-cooling holes". *ASME Journal of Turbomachinery,* **122**(1), pp. 146–152.
[14] Gritsch, M., Schulz, A., and Wittig, S., 2001. "Effect of crossflows on the discharge coefficient of film cooling holes with varying angles of inclination and orientation". *ASME Journal of Turbomachinery,* **123**(4), pp. 781–787.
[15] Gritsch, M., Schulz, A., and Wittig, S., 2003. "Effect of internal coolant crossflow on the effectiveness of shaped film-cooling holes". *ASME Journal of Turbomachinery,* **125**(3), pp. 547–554.
[16] Adami, P., Martelli, F., Montomoli, F., and Saumweber, C., 2002. "Numerical investigation of internal crossflow film cooling". In Proc. ASME Turbo Expo 2002, GT-2002-30171.
[17] Kissel, H., Weigand, B., Von Wolfersdorf, J., Neumann, S., and Ungewickell, A., 2007. "An experimental and numerical investigation of the effect of cooling channel crossflow on film cooling performance". In Proc. ASME Turbo Expo 2007, GT2007-27102, June, Montreal.
[18] Pietrzyk, J., Bogard, D., and Crawford, M., 1989. "Hydrodynamic measurements of jets in crossflow for gas turbine film cooling applications". *ASME Journal of Turbomachinery,* **111**(2), pp. 139–145.
[19] Leylek, J., and Zerkle, R., 1994. "Discrete-jet film cooling: A comparison of computational results with experiments". *ASME Journal of Turbomachinery,* **116**(3), pp. 358–368.
[20] Porter, J., Sargison, J., Walker, G., and Henderson, A., 2007. "Design and calibration of a facility for film cooling research". In Proc. 16th Australasian Fluid Mechanics Conference (on CD), December, Gold Coast, Australia.
[21] Wittig, S., Schulz, A., Gritsch, M., and Thole, K., 1996. "Transonic film-cooling investigations: effects of hole shapes and orientations". *ASME Paper No. 96-GT-222*.
[22] *CFX 11 Users Guide, 2008*. ANSYS Inc.
[23] Leedom, D. H., and Acharya, S., 2008. "Large eddy simulations of film cooling flow fields from cylindrical and shaped holes". In Proc. ASME Turbo Expo 2008, GT2008-51009, June, Berlin, Germany.
[24] Saumweber, C., and Schulz, A., 2008. "Free-stream effects on the cooling performance of cylindrical and fan-shaped cooling holes". In Proc. ASME Turbo Expo 2008, GT2008-51030, June, Berlin, Germany.
[25] Andreopoulos, J., and Rodi, W., 1984. "Experimental investigation of jets in a crossflow". *Journal of Fluid Mechanics,* **138**, pp. 93–127.